



Properties and phase structure of melt-processed PLA/PMMA blends

Mauricio Gonzalez-Garzon¹ · Shant Shahbikian¹ · Michel A. Huneault¹

Received: 5 September 2017 / Accepted: 3 January 2018 / Published online: 31 January 2018
© Springer Science+Business Media B.V., part of Springer Nature 2018

Abstract

This study examines the rheological, mechanical and thermal behavior of Poly(lactic acid)/Poly(methyl methacrylate) (PLA/PMMA) blends and takes a look at the phase structure evolution during their melt processing. Semi-crystalline or amorphous PLA grades were combined with PMMA of different molecular weight to prepare the blends. The rheological properties and phase structure was first assessed using small-amplitude oscillatory shear experiments. The blends were injection molded into bars and characterized in terms of their tensile properties and of their dynamic mechanical behavior. Differential scanning calorimetry was also used to study the miscibility and crystallization behavior of prepared blends. Tensile properties of the blends nearly followed a linear mixing rule with no detrimental effect that could have been associated with an uncompatibilized interface. However, dynamic mechanical analysis and calorimetric experiments showed that some phase separation was present in the molded parts. Nevertheless, a single T_g was found if sufficient time was given in quiescent conditions to achieve miscibility. The Gordon-Taylor equation was used to assess the polymer interactions, suggesting that miscibility is the thermodynamically stable state. The ability of PLA to crystallize was strongly restricted by the presence of PMMA and little or no crystallinity development was possible in the blends with more than 30% of PMMA. Results showed an interesting potential of these blends from an application point of view, whether they are phase separated or not.

Keywords Poly(lactic acid) · Polymethyl methacrylate · Miscibility · Phase structure

Introduction

Biobased polymers have become a valuable alternative to fossil-based polymers to prepare materials with a reduced carbon footprint and that are not dependent on petrochemicals. In this context, Poly(lactic acid), also known as polylactide or PLA, has been one of the most successful bioplastic in the last decade. It boasts a high tensile modulus and strength, it has a high transparency, it is fully biodegradable once hydrolyzed and it can be processed with the same equipment as other polyesters. Commodity PLA grades have mainly been serving the packaging markets where its biobased origin is valued by consumers and where its biodegradability offers the possibility of composting as an end-of-life option [1]. The life cycle of PLA packaging is relatively short since it is typically aimed at

the protection of fresh food products. Therefore, taking advantage of its good mechanical properties in longer life cycle engineering applications would be interesting. Additionally, increased use of PLA would give environmental benefits over current engineering materials since PLA production requires less fossil fuel and generates less greenhouse gases compared to most fossil-based engineering resins. Nevertheless, for longer-term applications, PLA has two major deficiencies. First, it suffers from a relatively low temperature resistance when used in its amorphous form due to its glass transition temperature occurring at around 60 °C. Secondly, PLA can suffer from hydrolysis in a hot and humid environment which is a serious issue when contemplating durable material applications. There is a whole window of opportunity in longer-term engineering applications that is nearly untouched for the moment greatly due to these deficiencies.

Polymer blending represents a practical and economical route to modify physical properties of polymeric materials, sometimes obtaining attractive novel properties which each individual material does not possess. Several polymers have been blended with PLA, typically with PLA as the major phase. Basic thermodynamics teaches us that two substances will be

✉ Michel A. Huneault
Michel.Huneault@usherbrooke.ca

¹ Department of Chemical and Biotechnological Engineering,
Université de Sherbrooke, 2500 Boulevard de l'Université,
Sherbrooke, QC J1K 2R1, Canada

miscible if the Gibbs free energy of the solution is smaller than the sum of the components free Energy. In terms of change in free energy, ΔG_m , this condition can be expressed from the enthalpy and entropy of mixing by the well-known Gibbs equation [2]. For polymer mixtures, the entropy of mixing is greatly reduced compared to small molecules due to the much lower number of conformations that can be taken by macromolecules. Since the enthalpy of mixing is generally small or positive, the vast majority of polymer pairs are immiscible. PLA based blends are no exception and PLA was shown to form immiscible blends with polyethylene [3], polypropylene [4], polystyrene [5], polyvinyl acetate [6], thermoplastic starch [7] as well as with other polyesters such as polybutylene succinate [8], polyhydroxybutyrate [9] and polyethylene terephthalate [10, 11]. PLA, however, can form partially miscible blends with polycaprolactone [12, 13], and with polyols such as polyethylene glycol (PEG) [14, 15]. The latter has a low glass transition and can be used to plasticize PLA.

PLA has been reported to be miscible also with polyacrylics, namely with poly(methyl methacrylate) or PMMA. Contrarily to PEG, PMMA has a much higher glass transition temperature than PLA and therefore, in this case, the miscible additive could improve the temperature resistance of a PLA-based material. Eguiburu et al. [16] were the first to investigate the miscibility of PLA / PMMA blends. They used dioxane as a common solvent to dissolve the polymers and carried out precipitation using hexane as a non-solvent. Interestingly, using differential scanning calorimetry (DSC) and dynamic mechanical analysis (DMA), the authors found that the solution/precipitation method lead to phase-separated blends (i.e. separate glass transitions) but that these blends became a single-phase mixture after heating to 200 °C and cooling back to room temperature. One interpretation may be that slight changes in precipitation sequence could generate separate phases in the solution precipitation step even if thermodynamics would favor a single-phase miscible system once the system was given sufficient time and mobility in the melt state. Zhang et al. using similar solvent and non-solvent later reproduced these results [17]. The authors, however, compared the precipitated blends to solvent casted ones and found that even after a thermal treatment, PLA and PMMA remained phase segregated. This pointed to the odd observation that miscibility, normally considered a strictly thermodynamic issue, was dependent on the dynamics of the solution mixing process.

Li and Woo published a thorough investigation of phase transitions for blends of PLA with PMMA of varying molecular weight and tacticity [18]. They prepared the blends by solvent casting using chloroform as a common solvent. Again, the as-cast samples of atactic PMMA/PLA blend exhibited two T_g that changed into a single transition after a thermal treatment. The authors interpreted this behavior as an indication that the blend had an upper critical solution temperature (UCST) which means that the blend undergoes an immiscible-

miscible transition once it is heated above a certain critical temperature. Rapidly cooling the samples from the miscible state resulted, according to the authors to a quasi-miscible state in which the polymer blend was “frozen” into a single phase. This interpretation helped to explain the transition from immiscible to miscible observed by calorimetry after a thermal treatment. Determination of the UCST were made observing the clarity of the samples with an optical microscope at elevated temperatures. The UCST was shown to systematically increase with PMMA molecular weight and with PMMA weight fraction in the blend. In a separate work, Li and Woo also showed that the blend’s UCST was influenced by PMMA’s tacticity [19]. The use of syndiotactic PMMA led to similar results than those obtained with the atactic PMMA. By contrast, blends of isotactic PMMA with PLA seemed to remain phase separated. The authors suggested that small differences in solubility parameters when changing from atactic to isotactic PMMA may explain the change in solubility. It is noteworthy however that the isotactic and syndiotactic PMMA used in this investigation differed widely in terms of their average molecular weight (50 kg/mol and 300 kg/mol respectively). Since dynamics seem to play a role in the phase separation, it is possible that the lower molecular weight i-PMMA was able to phase separate more readily because of its greater fluidity while the high molecular weight s-PMMA could be frozen in the quasi-miscible state despite slightly unfavorable thermodynamics.

Several authors further investigated the relation between the phase behavior and the preparation method leading to contradictory conclusions. Shirahase et al. [20] reported an homogeneous single T_g material when melt-blending PLA and PMMA using a two-roll mill. Conversely, Le et al. [21] reported phase-separated co-continuous morphologies for blends prepared using single screw extrusion. Anakabe et al. [22] reported immiscibility for blends prepared using a twin screw extruder but confirmed the earlier finding that in calorimetric experiments, a single glass transition temperature can be observed in a second heating cycle. Samuel et al. [23] compared the phase behavior of the same blends prepared by melt-processed and by solvent casting. They reported that the melt-mixed blends were homogeneous while the solvent-casted ones were phase separated. Furthermore, seemingly miscible blends were able to phase separate when re-dissolved in a common solvent. All these contradicting information point to a single conclusion: that the observed homogeneous state is not truly an equilibrium state and therefore that from a purely thermodynamic point of view, the blend is not fully miscible. It phase separates slowly however and therefore the blend can be observed in a single-phase state before any separation occurs.

One particular feature of the PLA/PMMA blend is that the PLA has the ability to crystallize if it is of sufficient optical purity (i.e. high *L*-Lactic acid content). In such blends, the

concept of miscibility is restricted to the miscibility of the amorphous phase of the crystallisable polymer with the other amorphous polymer. The presence of the amorphous polymer is known to cause a melting point depression that can be used to estimate the interaction parameter between the two polymers χ_{12} , using the basic relationship from Flory-Huggins equation [24]. Using this approach, the interaction parameter for the PLA-PMMA pair was shown to be slightly negative: $\chi_{12} \approx -0.2$ [19, 25]. This enthalpy of mixing is directly linked to the interaction parameter in the Flory-Huggins theory [2]. A slightly negative χ_{12} leads to a negative enthalpy of mixing and thus supporting, like Li and Woo, the thermodynamic of forming a miscible blend especially at high temperature. Another consequence of the addition of PMMA was to greatly reduce the crystallization rate. This was shown through direct spherulite growth rate measurements by Canetti et al. [25].

From the literature review, the current understanding is that subjecting the blend to melt-mixing or even simply to elevated temperature in quiescent conditions can lead to a seemingly homogeneous, transparent, single- T_g material. The next questions that need to be addressed are on the necessary melt-mixing conditions required to generate a single-phase, on the conditions that may lead to phase separation and on the potential of these blends from an application point of view, whether they are phase separated or not. In the current investigation, PLA/PMMA samples were prepared by injection-molding, a common industrial melt-processing technique, with the aim to investigate the resulting phase structure, to assess the processability and to determine thermal and mechanical performance of these blends. Since crystallization could be a means to improve thermal resistance of the material, a particular emphasis was also placed on the effect of the material selection on the ability of the blend's PLA to crystallize.

Experimental

Materials

Three grades of PLA supplied by NatureWorks LLC were used. In increasing order of optical purity and thus of ability to crystallize, the grades were Ingeo™ 6060D, 4032D and 3100HP. These comprise respectively around of 88, 95 and 98 wt% of L-lactic acid content and were selected to assess how PLA grade selection can influence PLA crystallization and the blends final properties. We will refer to the grades, respectively as the *a*-PLA, *c*-PLA, *hc*-PLA where the letter *a* refers to the amorphous nature, *c* to the semi-crystalline nature and *hc* refers to the higher purity and higher crystallization ability of the latter grade. For the acrylics, two grades of PMMA supplied by Arkema were used: Plexiglass® V826 and V920. Both of them were homopolymers but they differ in terms of melt viscosity due to their different molecular weight. They will be referred to as the high and low

viscosity grades and thus as *hv*-PMMA and *lv*-PMMA respectively. Throughout this paper, concentrations will be given in weight percent.

Processing

Before processing, the PLA and PMMA were dried overnight under vacuum at 50 °C, to reduce the humidity and avoid PLA hydrolysis at high temperatures. Six different polymer pairs of PLA and PMMA with different compositions (100/0, 90/10, 70/30, 50/50, 30/70, 10/90, 0/100) were melt blended in the mixing unit of a vertical injection machine Mini-Jector #55P-2. The blending was carried out keeping the barrel temperature of the mixing unit at 230 °C. The injection was carried out using an injection pressure of 6 MPa into a room-temperature ASTM Type-I tensile test bars mold. A total cycle time of 45 s was used. In selected experiments, a dwell time was added between the mixing step (i.e. melt-mixing in the extrusion unit) and the mold injection step to enable additional molecular chain diffusion in the blends.

Characterization

Rheological properties

The rheological characterization of the different polymers and blends was carried out in the oscillatory shear mode at 200 °C using a 25 mm plate-plate geometry in an Anton-Paar MCR-502 rheometer. The sample disks (25 mm diameter, 1 mm thick) were prepared by compression molding. A strain amplitude between 5 and 10% was used for all oscillatory experiments over the frequency range of 0.1 to 300 rad/s. Before molding samples and before rheological measurements, materials were dried under vacuum at 50 °C for a minimum of 12 h to remove humidity. The rheometer testing chamber was maintained under a nitrogen flow to minimize degradation of the polymers.

In order to verify the crystallization under shear, some selected samples were cooled from 190 °C to different crystallization temperatures (130, 140 and 150 °C) using a Peltier plate at a rate of 20 °C/min. Time sweep tests were then carried out at a constant frequency of 0.628 rad/s at the aforementioned isothermal conditions.

Mechanical properties

Tensile tests were performed using an Instron 4202 tensile testing machine on ASTM type I tensile specimens. The cross-head speed was 1 mm/min and the load was measured using a 10 kN cell. A contacting axial extensometer Epsilon 3442 was used to precisely monitor the initial deformation rate. The specimens were conditioned for at least 48 h at room temperature after their molding. Reported values are the averages obtained over at least seven measurements.

Dynamical mechanical analysis (DMA)

DMA analysis was carried out using a PerkinElmer DMA 8000 in a dual cantilever bending mode with an amplitude of 50 μm at a frequency of 1 Hz. Storage and loss modulus were determined as a function of temperature from 30 to 150 $^{\circ}\text{C}$ at a heating rate of 3 $^{\circ}\text{C}/\text{min}$. Bars of $50 \times 10 \times 3$ mm were used for the DMA testing. These bars were cut out of the central section of injection molded tensile specimens using a sliding microtome Leica SM2500.

Differential scanning calorimetry (DSC)

Thermal characterization was performed on 10 mg samples using a TA Instrument Q-1000 DSC under nitrogen flow. The samples were heated at 10 $^{\circ}\text{C min}^{-1}$ from -10 $^{\circ}\text{C}$ to 200 $^{\circ}\text{C}$ to erase thermal history, cooled at 5 $^{\circ}\text{C}/\text{min}$ to -10 $^{\circ}\text{C}$, and heated again at 10 $^{\circ}\text{C}/\text{min}$ to 200 $^{\circ}\text{C}$. The cooling and second heating scans were used to evaluate the material's ability to crystallize and the thermal transition temperatures. Crystallinity values were calculated based on only the PLA fraction and used an enthalpy of fusion of 93 J/g for 100% crystalline PLA [26].

Results and discussion

Melt-state rheology

The first step in the preparation of PLA/PMMA parts is the melt-mixing. Melt rheology is therefore of interest to characterize the fluidity of our materials and as a means to assess the phase structure of the blends in the melt state. As a reference, the complex viscosity of the neat polymers is presented in Fig. 1 as a function of frequency. The first striking difference is that the three PLA grades differ greatly from the two PMMA both in terms of the viscosity levels and of the viscosity curve shape. PMMA had a zero-shear viscosity that was 2 orders of magnitude higher than that of PLA and a longer transition zone between the Newtonian behavior and the terminal Power-Law region. By contrast, PLA exhibited a much lower dependence on frequency and was characterized by a well-defined Newtonian viscosity plateau within the 200–300 Pa.s range. Even if this is not emphasized by the wide viscosity range of the figure's ordinate, it is noteworthy that the hv-PMMA was around 5 times more viscous, at low frequency, than the lv-PMMA.

Figures 2, 3, and 4 present the blends' rheological behavior after injection molding. Figure 2 displays the typical complex viscosity η^* as a function of angular frequency for the c-PLA/hv-PMMA blends at 200 $^{\circ}\text{C}$. A regular increase in viscosity was observed as the PMMA content of the blend was increased. The transition between the plateau viscosity and the

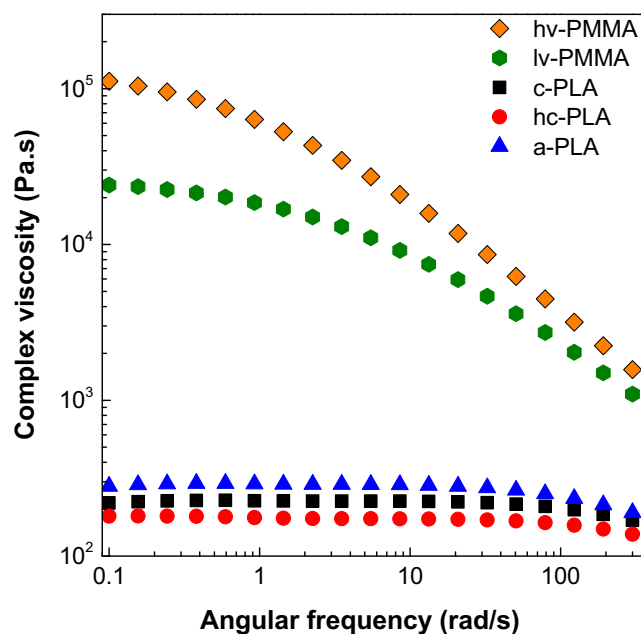


Fig. 1 Complex viscosity as a function of frequency of pure c-PLA, hc-PLA, a-PLA, hv-PMMA and lv-PMMA at 200 $^{\circ}\text{C}$

shear-thinning region was also progressively pushed to lower frequency indicative of an increase in the material's relaxation time. Similar results were obtained with the other polymer pairs. One key point from a practical point of view for the use of this blend is that the overall material viscosity can be drastically reduced by the addition of PLA to PMMA. Even at high frequency (100 rad/s), typical of processing conditions, where the viscosity are more closely grouped, the addition of 10% PLA could reduce the viscosity by over 25% and the use

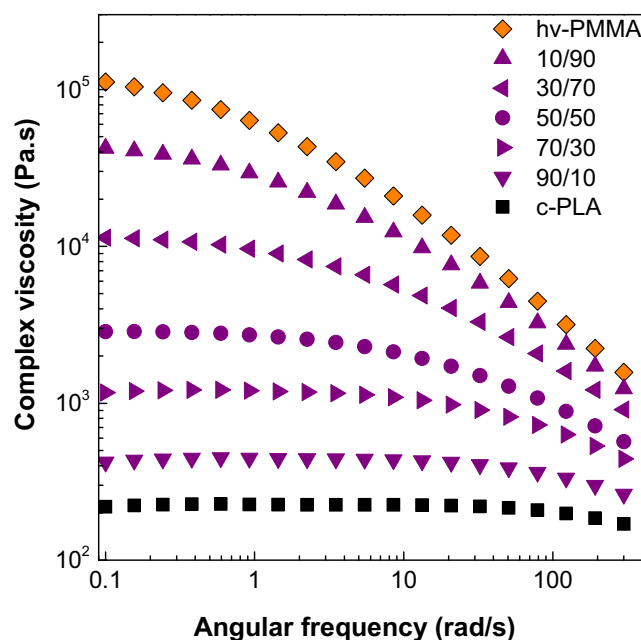


Fig. 2 Complex viscosity of hv-PMMA/c-PLA blends as a function of frequency at 200 $^{\circ}\text{C}$

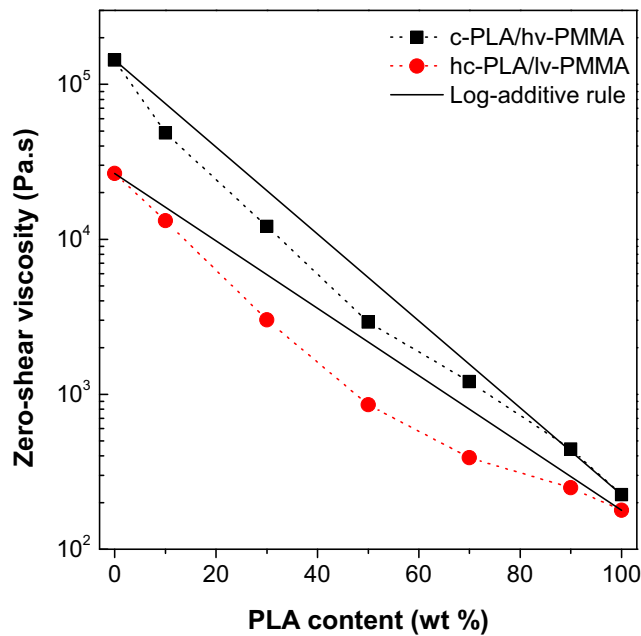


Fig. 3 Newtonian plateau viscosity as a function of PLA content of c-PLA/hv-PMMA and hc-PLA/lv-PMMA blends

of 30% PLA could half the material viscosity. Since both materials have similar tensile strength and modulus, this opens the path to more processable materials with potentially little or no cost in material properties. This contrast with the trade-off often encountered between properties and processability when selecting a lower molecular weight resin to improve moldability. This will be discussed further when analyzing the tensile properties of the blends.

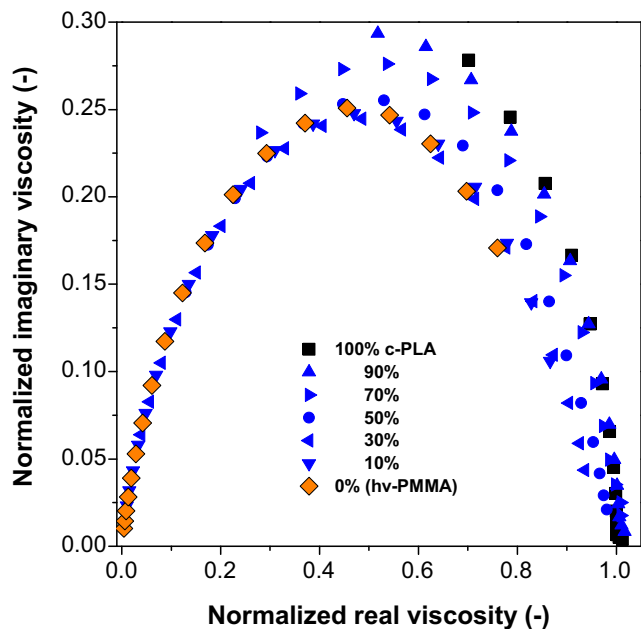


Fig. 4 Normalized Cole-Cole plot, i.e. imaginary viscosity (η''/η_0) as a function of the real viscosity (η'/η_0) vs for c-PLA/hv-PMMA blends at 200 °C

The plateau viscosities were measured directly for PLA-rich blends. For PMMA and PMMA-rich blends, it was obtained by curve-fitting the data using the Carreau-Yasuda viscosity equation. The zero-shear viscosity data is summarized in Fig. 3 as a function of the PLA content. The observed data closely followed a log-linear mixing rule with only a slight negative deviation. The literature on polymer blend rheology is not straightforward and a large range of behavior has been reported depending on the blend systems. Even though, positive or negative deviations have been reported, there is a consensus that a log-linear relationship is, a priori, expected from a single phase mixture. By contrast, in a dual phase blend, the matrix tends to control the blend’s viscosity at low dispersed phase concentration leading to a sigmoidal viscosity-composition curve. Also, the establishment of a co-continuous morphology near the phase inversion concentration can also lead to large deviations compared to the log-linear rule. For example, Roovers et al. [27] reported linear dependence of $\log(\eta_0)$ on composition for some miscible polymers pairs and several other authors showed a transition between positive and negative deviations from additive rule associated to phase inversion in immiscible systems [28–30]. Therefore, the observed behavior in the PLA/PMMA blends could be associated to one of a miscible system.

Another indication of miscibility in a system is the presence of a single relaxation mechanism. This verification is often made using a representation known as the Cole-Cole plot where the imaginary part of the complex viscosity (η'') is plotted as a function of its real part (η') [31, 32]. Figure 4 presents normalized Cole-Cole plots for c-PLA/HV-PMMA blends at 200 °C. Considering the huge differences in the viscosity values from blend to blend, the real and imaginary viscosities were normalized by dividing them by their corresponding zero-shear viscosity. All experimental results followed a circular pattern on the plot. Such a circular trace without any tail or a secondary circle is indicative of a single relaxation mechanism in the system and therefore supports the idea that the blend is miscible in the melt state. Similar results were obtained for all PMMA/PLA pairs.

Mechanical and thermal resistance

Once the blends have been melt mixed in what was seemingly a single phase, they have been injected into a mold and cooled to their glassy state. The room-temperature mechanical behavior of all blend combinations was examined through standard tensile testing. To represent the large body of experimental data in a unified fashion, it was decided to compare the results in relative terms. In particular, the tensile modulus and strength will be presented in terms of their deviation compared to a linear mixing rule. Figure 5 thus presents the deviation from the additive rule for Young’s modulus and tensile strength of different PLA/PMMA systems. In absolute terms,

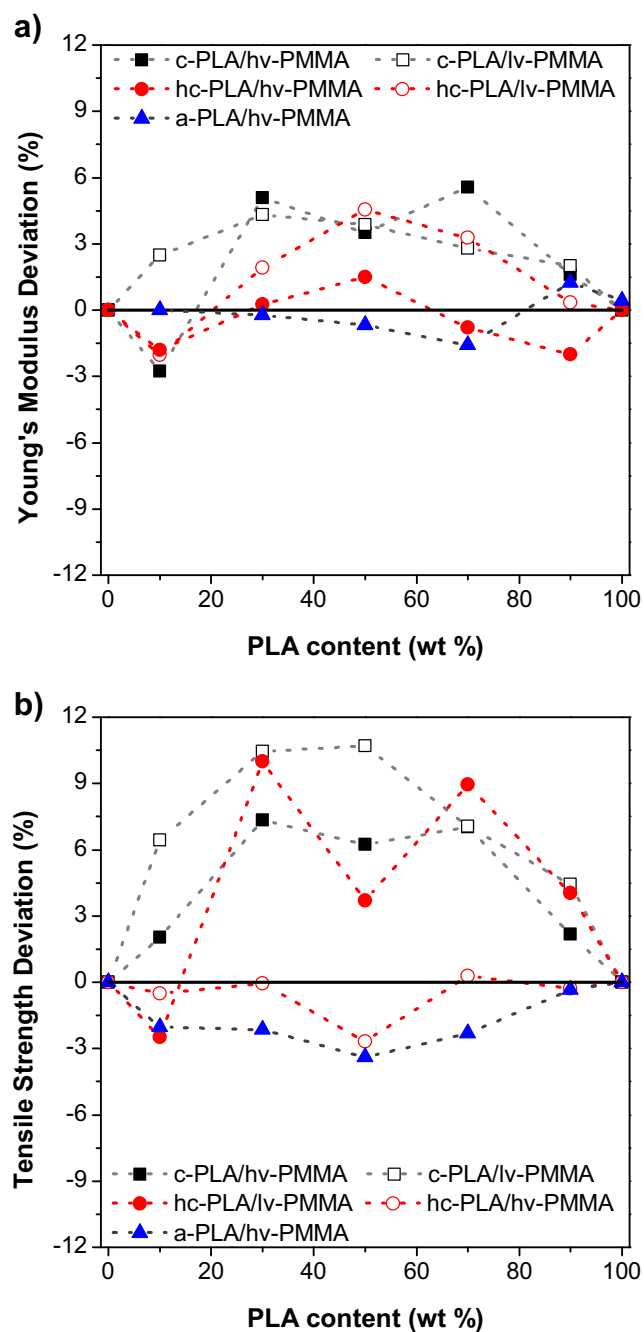


Fig. 5 Mechanical properties for different PLA/PMMA systems. Deviation from linear additive rule for a) Young's Modulus, and b) Tensile Strength

the Young's modulus for pure PMMA and pure PLA were respectively close to 3.2 and 3.5 GPa with little variation with regards to the grade. The measured deviations from the mixing rule were slightly positive but the deviations were at most +6%. No particular trend could be identified in relation to the blend combinations.

The tensile strength for pure materials was 73 and 63 MPa respectively for pure PMMA and pure PLA. The deviation from the linear mixing rule was also

relatively small with maximum deviation again being positive and within +11% of the value predicted by a linear mixing rule. The measured deviation again could not be associated to a particular cause in terms of polymer grade combination. It is quite striking that all data for modulus and strength was either close to the linear mixing rule (i.e. 0% deviation) or slightly above. The tensile modulus is measured at initial deformation and is typically not highly interface dependent. A linear mixing rule could therefore be reasonably expected. The slight positive deviation is surprising and shows that interactions between PLA and PMMA macromolecules are as strong as the self-interaction. Tensile strength by contrast is typically very sensitive to state of the interface since any lack of adhesion between two phases translates into debonding and reduction of stress transfer when the stress in the material exceeds a critical interfacial resistance. Therefore, the positive tensile strength deviation is again indicative of either the absence of interface or that if an interface is present; it is just as strong as the cohesive strength of the pure materials and possibly increases the resistance of the major phase through confinement or surface orientation effects. These results seem to indicate a good application potential for these blends especially if we combine them with the earlier finding that hinted at a dramatic improvement in moldability due to the materials' viscosity reduction (compared to the use of pure PMMA).

The tensile data was obtained at room temperature. As a next step to verify the blends' potential, it was interesting to investigate how the materials rigidity could evolve with temperature. The blends were therefore subjected to a dynamic mechanical solicitation to monitor their response as a function of temperature. Figure 6 presents the storage modulus of the materials as a function of temperature as measured in dual cantilever DMA mode. As expected, all blends and pure components present a glassy plateau at low temperature followed by a rapid drop in the storage modulus associated with the glass transition of the polymer. In standardized material testing, the heat distortion temperature (HDT) is measured by subjecting a sample to three-point bending while temperature is raised at a constant rate. The HDT is the temperature at which a certain critical deflexion is reached. The dynamic mechanical analysis data can be interpreted in the same fashion by comparing the temperature associated to a given storage modulus value. If 1 GPa is selected as this modulus value, it can be noted that the temperature resistance, noted as T_{1GPa} , increased progressively from 58 °C for pure PLA to 62 °C with 30% PMMA and up to 68 °C and 74 °C for blends containing 50 and 70% PMMA, respectively. This shows that thermal resistance of PLA can be improved with the addition of PMMA and could be tailored depending on the application requirements.

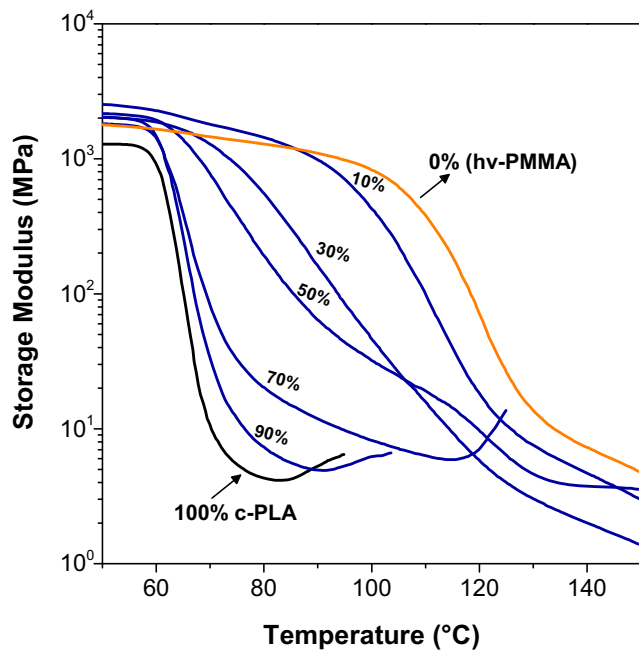


Fig. 6 Storage modulus as function of temperature for c-PLA/hv-PMMA blends

Phase behavior

The dynamic mechanical analysis can also be used to determine thermal transitions by monitoring the tangent of the phase angle, $\tan \delta$, between the measured stress and the applied deformation. The $\tan \delta$, also known as the damping coefficient, is the ratio between the viscous and elastic parts of the complex modulus and it reaches a maximum in the vicinity of the glass transition temperature. Fig. 7 shows $\tan \delta$ as a function of temperature for c-PLA/hv-PMMA blends for two blend preparation techniques. For Fig. 7a, the blends were melt mixed in the plasticizing unit of the injection molding while for Fig. 7b, the materials were first melt-mixed in an internal mixer and then compression molded. For both preparation methods, the pure materials exhibited single $\tan \delta$ peaks at around 68 °C and 125 °C for pure c-PLA and hv-PMMA respectively. A single $\tan \delta$ peak is typical of a single-phase material.

By contrast, the results for the blends produced by injection molding were more complicated. At 30% PLA, a single but very wide peak was observed while at 50 and 70% PLA, two peaks were noted with each peak being shifted toward intermediate temperatures. Therefore, this seems to indicate that, even though one component was able to partially dissolve in the other and influence its glass transition, the material as a whole did not yet form a single phase. Fig. 7b, present the $\tan \delta$ vs temperature data for the same blends that were melt-mixed in an internal mixer rather than in the plasticizing unit of an injection molding machine and compression molded rather than injection molded. Surprisingly, when using this processing sequence, single and sharper peaks were observed for the 30 and 50% PLA blends

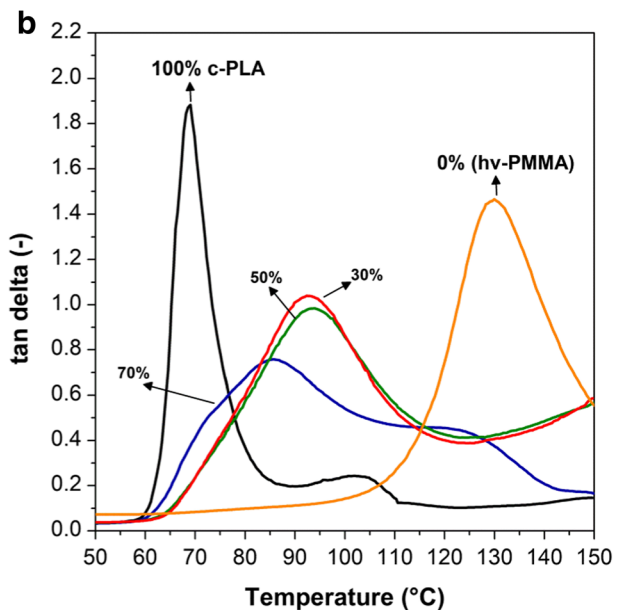
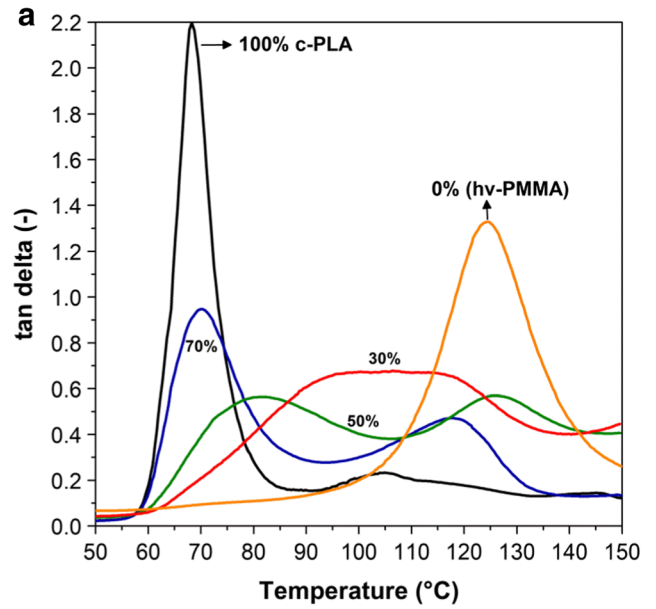


Fig. 7 $\tan \delta$ profiles for c-PLA/hv-PMMA blends a) Injection molded (no dwell time), and b) melt-mixed for 10 min and compression molded.

while the 70% blend still maintained shifted but distinctive peaks for each phases. The difference observed for similar blend compositions when changing the processing sequence suggests that the dynamics, and therefore, the kinetics of the dissolution should be taken into consideration whenever examining the phase behavior of the PLA/PMMA blend. Even though the miscibility of a blend is strictly a thermodynamic phenomenon; the process of solubilization (as well as the phase separation) is not instantaneous and can therefore be controlled by process dynamics.

Since inter-diffusion of the polymer chains seemed to be an important parameter, the c-PLA/hv-PMMA 50/50 blend was used to produce injection molded parts adding a dwell time between the melt-mixing and the injection step (i.e. in the

plasticizing unit of the injection molding machine). This dwell time, ranging from 0 to 20 min, allowed quiescent inter-diffusion prior to the injection step. The molded samples were then subjected to DMA testing to monitor changes in the $\tan \delta$ versus temperature curves, reported in Fig. 8. The sample molded without delay exhibited the two clear peaks and these two peaks shifted toward an intermediate temperature with increasing the dwell time. Only samples held for 20 min in the quiescent melt state exhibited a single peak. By contrast, a sample melt-mixed for 10 min in an internal mixer and then compression molded also exhibited a single peak indicating that dynamic mixing conditions favored the solubilization dynamics, as expected. It shows that the plasticizing unit of an injection molder does not lead to the equilibrium single phase by lack of time and mixing. This could be improved by the use of a mixing screw in the plasticizing unit or by a prior compounding step.

The phase transition of the prepared blends was also studied by differential scanning calorimetry (DSC). DSC is complementary to DMA since it is based on a different principle (i.e. heat flow vs viscoelastic response) and also allows to probe the sample using a more complex thermal history including cooling from liquid-state and second heating. Figure 9 presents the first heating, cooling and second heating scans for c-PLA/hv-PMMA blends. The first heating scan (Fig. 9a) enabled to probe the material in the state in which the samples were molded. In this first heating, c-PLA presented a T_g around 61 °C followed by a broad cold crystallization exotherm centered around 110 °C and a melting endotherm peaking at 176 °C. The blends exhibited melting endotherms of decreasing intensity with PMMA concentration up to 50% and no peaks at all in the blends where PMMA was the major component. The initial sample crystallinity was

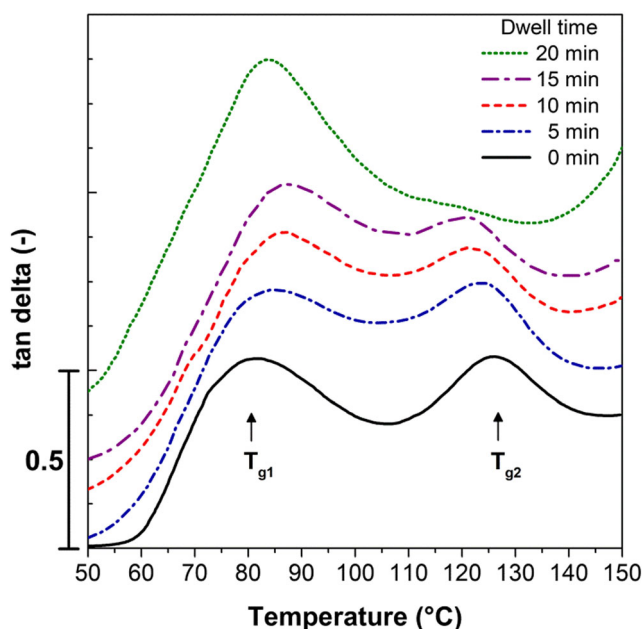


Fig. 8 Influence of dwell time on evolution of $\tan \delta$ for injection molded c-PLA/hv-PMMA blends

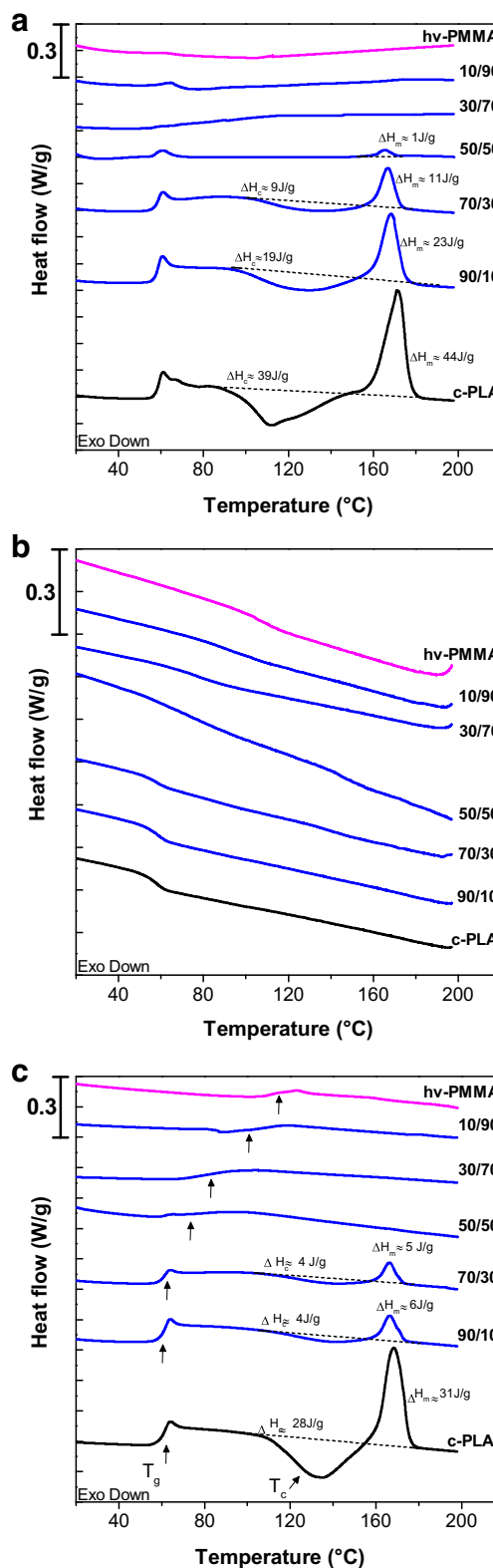


Fig. 9 DSC thermograms for (a) first heating, (b) cooling and (c) second heating scan for c-PLA/hv-PMMA blends. Heating scans were performed at 10 °C/min and cooling scan at 5 °C/min

estimated by subtracting from the melting endotherm the total energy released by the sample in the cold crystallization

endotherm. At all concentrations, this lead to the conclusion that the molded samples were almost fully amorphous after molding. The T_g associated with the PLA phase remained visible and did not shift much with the addition of PMMA supporting the idea that a PLA rich phase was still present. A second transition associated to a PMMA rich phase was more difficult to detect because it overlapped with PLA crystallization. Upon cooling (Fig. 9b) and upon second heating (Fig. 9c), the glass transition became better defined. No crystallization was observed in the materials upon cooling. Upon second heating, a single glass transition was observed and the T_g clearly increased with PMMA content. For example, it reached 65 °C when 30% PMMA was present and up to 85 °C with 70% PMMA.

With increasing PMMA content, PLA’s ability to cold crystallize was also systematically reduced and the crystallization endotherm shifted to higher temperatures. Restriction in PLA cold crystallization can be explained by the increase in the blend’s T_g that reduces the chain mobility but also to the intrinsically higher viscosity of the PMMA which also reduce the mobility of the PLA chains that are in the process of chain folding and re-organizing into a crystal lamellae. The peak melting temperature of the produced crystal phase shifts very slightly to lower temperature with the addition of PMMA. Melting temperature depression is expected for miscible blends with a positive Flory-Huggins interaction parameter as explained in the introduction.

Another noteworthy feature was the widening of the glass transition defined as the temperature window between the onset and the end of the transition. This broadening in transition was also noted in DMA tests where the $\tan \delta$ peak intensity decreased with increasing PMMA content, indicating some modifications in the mobility of the amorphous phase by the presence of PMMA. Table 1 summarizes the transition temperature and transition width measured by DMA and DSC. In calorimetric measurement, the transition occurred over a range of 4 °C for pure PLA and over 11 °C for pure PMMA. For the 30 and 50% PLA blends, the transition width was much greater extending over 24

and 29 °C respectively. In DMA, transition width was calculated at half of the peak maximum. Transition width for pure materials was in agreement with those detected by DSC. Also, the broadest transition was recorded at 30% of PLA. As expected, for those injection molded blends where phase separation was evidenced, the width of each peak was similar to the width of the pure material’s peak. It is interesting to notice how in the 50/50 injected molded blend, the peak width corresponding to PLA-rich phase was greatly widened (to 14 °C) although the blend was phase separated. It reveals that the PLA-rich phase has a wide concentration distribution caused by local heterogeneity at a macromolecular scale. This could be explained by the “self-concentration model” for miscible blends developed by Lodge and McLeish [33]. According to the “self-concentration” approach, the chain mobility of the lower T_g material tends to stay close their pure state chain mobility, whereas, for the the higher T_g material, the chain mobility increases as if it sensed more a blend average mobility. The consequence is that the glass transition broadness is greater when the blend is richer in the higher T_g material leading to an asymmetrical situation. In the current study, PMMA is the high T_g material and one can notice that the transition broadness is greater for the PMMA rich blends. Moreover, the greater difficulty in dissolving PMMA into a PLA major phase leads to phase separated blends (i.e 10 and 30% PMMA blends). Conversely, the higher mobility PLA chains are easier to solubilize in PMMA leading to a single phase at the complementary concentration (i.e. 10 and 30% PLA blends).

Figure 10 presents the second heating scan but this time with both the high crystallinity and the amorphous PLA grades, i.e. with hc-PLA and a-PLA. These polymer pairs were investigated to determine if PLA’s optical purity or ability to crystallize alter the phase behavior of the blend. For both blend series, the T_g was unique and shifted with composition in a very similar fashion as for the c-PLA/PMMA series. Obviously, for the amorphous grade no crystallization occurred. For the hc-PLA/PMMA blend series, the crystalline behavior exhibited only some subtle differences. The pure hc-PLA crystallized more

Table 1 Glass transition temperature and transition width for c-PLA/hv-PMMA blends

% PLA	T_g (°C)				Transition width (°C)			
	DSC		DMA		DSC		DMA	
	2nd heating		Injection molded	Compression molded	2nd heating		Injection molded	Compression molded
100	61	68	–	69	4	4	–	4
90	62	69	115	n.d	4	6	11	n.d
70	65	70	118	84	7	6	10	15
50	73	81	124	92	29	14	12	15
30	85	105	–	95	24	28	–	18
10	104	117	–	n.d.	18	15	–	n.d.
0	112	125	–	130	11	11	–	11

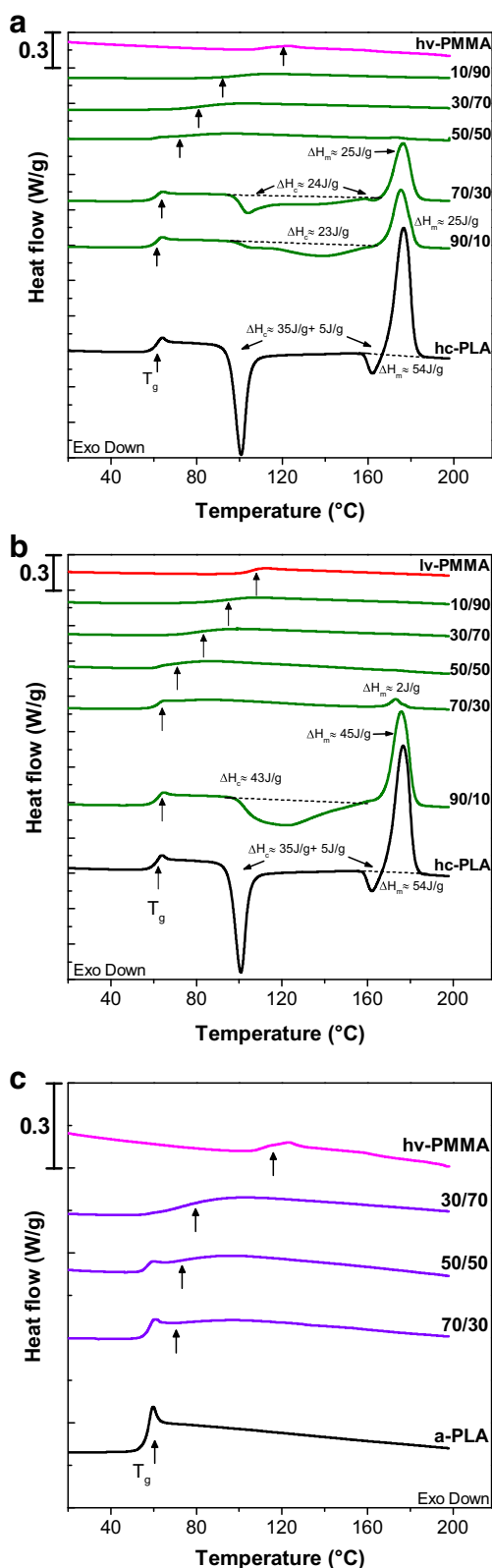


Fig. 10 DSC thermogram for second heating scan of (a) hc-PLA/hv-PMMA, (b) hc-PLA/lv-PMMA, and (c) a-PLA/hv-PMMA blends

readily with a sharp cold crystallization centered around 100 °C. At this crystallization temperature, PLA is known to form the so-

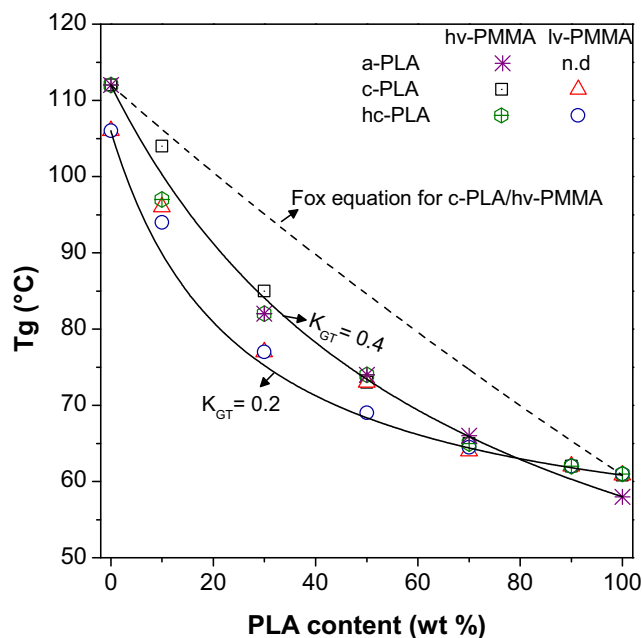


Fig. 11 Glass transition temperature as a function of PLA content. Gordon-Taylor Equation predictions (solid lines) and Fox Equation predictions (dash line)

called α' crystals that tend to transform into the more stable α form by melt recrystallization or solid-solid transition prior to the melting endotherm. This explains the separate exotherm around 160 °C, suggesting that in the current conditions, the PLA partially crystallize in the α' form. These features did not lead to any dramatic increase in crystallization in the blends however and again crystallization was fully inhibited as soon as the

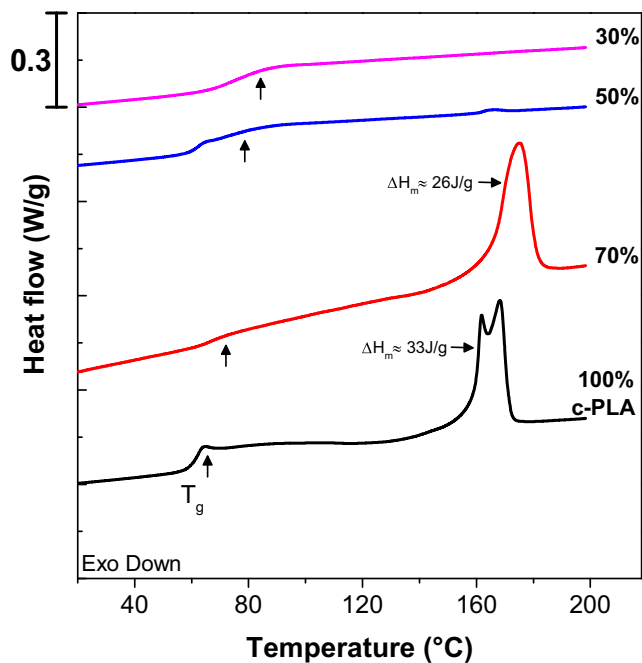


Fig. 12 DSC thermogram of c-PLA/hv-PMMA system after annealing for 30 min at 110 °C

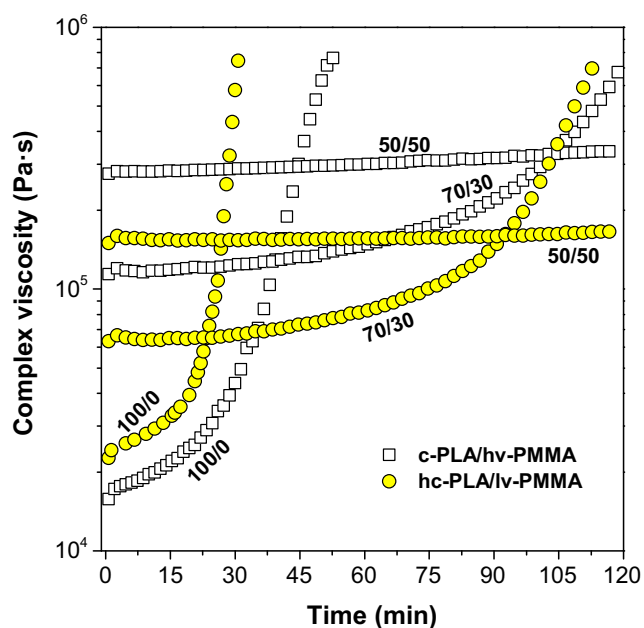


Fig. 13 Complex viscosity evolution at 130 °C and 0.628 rad/s for c-PLA/hv-PMMA and hc-PLA/lv-PMMA blends

50% PMMA level was reached. At 10 and 30% PMMA, the melting endotherms were slightly sharper and of higher magnitude but the initial crystallinity were all close to zero. Thus, there wasn't any significant crystallinity developed during cooling even though a slow cooling rate of 5 °C/min was used. This shows that it would be difficult to generate crystalline parts in an industrial molding cycle where cooling rates are several orders of magnitude greater.

Dependence of T_g on composition was analyzed using classic predictions from the Fox and Gordon-Taylor equations [34]. The Fox equation considers an ideal blend assuming similar specific volume for the two components, while the Gordon-Taylor enables to consider specific interaction through modification of an empirical parameter k_{GT} . The Fox and Gordon-Taylor equation can respectively be written as:

$$\frac{1}{T_g} = \frac{w_1}{T_{g1}} + \frac{w_2}{T_{g2}} \tag{1}$$

$$T_g = \frac{w_1 T_{g1} + k_{GT}(w_2) T_{g2}}{w_1 + k_{GT}(w_2)} \tag{2}$$

where T_{gi} denotes glass transition temperature of the pure component, i.e. 1 and 2, w_i is the weight fraction of component i. The k_{GT} parameter value depends on the change in thermal expansion coefficient of the components as they change from the glassy to rubbery form. If k_{GT} is set to a value of T_{g1}/T_{g2} , the Gordon-Taylor reduces to the Fox Equation, and in the limiting case where $k_{GT} = 1$, equation 2 is reduced to a linear additivity rule. Figure 11 displays the measured glass transition temperature along with predictions from the theoretical equations. In all cases, the measured glass transition

temperature was lower than the Fox equation predictions, indicating a negative deviation. A good agreement was obtained for each pair using different Gordon-Taylor parameter k_{GT} from 0.2 corresponding to hc-PLA/lv-PMMA system to 0.4 for a-PLA/hv-PMMA pair. The k_{GT} value can be considered as a measure of the interactions strength between components in the blend. Low values of k_{GT} have been interpreted as a weak interaction between polymer chains, in this particular case, between the ester carbonyl of PLA and the acrylic carbonyl of PMMA [19]. That assumption is in agreement with the transition broadness observed for all PLA/PMMA systems evaluated in the present work and, can suggest that we are dealing with systems that are close to the solubility limit.

Separate annealing tests were made on selected PLA/PMMA samples to investigate if crystallization and phase separation could be induced. Figure 12 displays the DSC curves upon second heating of c-PLA/hv-PMMA after annealing at 110 °C for 30 min. The pure c-PLA crystallized during thermal treatment and showed two clear melting endotherm around 168 and 173 °C, upon re-heating. The endothermal peak corresponds to a crystallinity fraction $X_c = 35\%$. These melting peaks are assigned to the melting of α' and α crystals [35]. When 30% PMMA was added, crystallinity was reduced, but annealing enabled the PLA phase to reach a crystalline fraction of 28%. Blends with 50% and 70% PMMA did not exhibit any significant endotherm peak indicating that they remained completely amorphous even after a 30 min annealing at 110 °C.

It is experimentally difficult to monitor real-time crystallization of slowly crystallizing materials by calorimetry since the exothermic heat flow rates may become small and cannot be accurately measured. An alternative way to determine the onset of crystallization is to monitor the rheological response over time. Since the onset of crystallization can be seen as a physical crosslinking between amorphous chains, it has a tremendous effect on the viscoelastic properties of a polymer. This technique has been used before, for example, to monitor small exothermic changes related to PLA stereocomplexation [36]. Annealing tests were therefore carried out under small-strain oscillatory shear. Figure 13 presents the evolution of complex viscosity for pure PLA, for c-PLA/hv-PMMA and for hc-PLA/lv-PMMA blends at 130 °C. For pure c-PLA and pure hc-PLA, crystallization is evidenced by the increase in melt viscosity observed over the duration of the test. In fact, their viscosity was never at steady-state indicating that crystallization had already begun at the start of the rheological monitoring. For blends with 30% PMMA, a viscosity plateau was first observed followed by a gradual increase in complex viscosity. The plateau region, that can be referred to as the crystallization induction period is, for both blend series, very long, in the order of 45–60 min. At 50% PMMA, the complex viscosity was stable over the 120 min of the experiment. Thus, to all practical purposes, the 50% PMMA blend cannot be

crystallized even using long annealing times and a temperature that is typically favorable to PLA crystallization. It is noteworthy that pure PLA does not have a wide crystallization window compared to other common polymer because it has a relatively high T_g and low melting temperature. The addition of PMMA, by increasing the T_g of the material further reduced the chain mobility in the typical temperature window for PLA crystallization. This comes at the same time with a reduced driving force for crystallization because of T_m reduction and lower enthalpy gain. This means that crystallization cannot be used as an additional means to improve the temperature resistance of the blend. However, it boasts the advantage of preserving the transparency of the material.

Conclusions

Phase behavior, thermal, mechanical and rheological properties of PLA/PMMA blends were investigated. It was found that the blends can be transformed into a single phase material but that a sufficiently long blending period is necessary to homogenize the blends. This explains literature's contradicting results reported in studies that used different blending protocols. The single-phase behavior in the melt state was supported by nearly additive blend viscosity as a function of composition and by examining Cole-Cole plots that showed the typical behavior of a single-phase system. Calorimetric data showed that a quiescent heating/cooling was sufficient to transform a seemingly 2 two phase system (2 separate T_g) into a single T_g material. The very wide glass transitions were however indicative of a wide composition distribution that could be interpreted as sign of imminent separation. In terms of tensile modulus and strength, the properties were also very close, but always slightly superior, to those predicted by a linear mixing rule. This confirmed that PLA and PMMA are very compatible in the solid state, even if some phase separation was observed by dynamic mechanical analysis.

In terms of processing, the large viscosity mismatch between commercial PMMA and PLA grades opens the path toward important improvement in PMMA processing. This difference is due to intrinsic polymer properties, namely to their chain entanglement characteristics. The positive practical consequence of this mismatch is that addition of PLA to PMMA can dramatically decrease the viscosity of the material thus facilitating its processing in the injection molding process, enabling for example the filling of thinner parts or better replication of fine mold details. It is noteworthy that this enhanced processability does not come at any expense in mechanical terms since as noted above, the blends showed higher modulus and tensile strength than what was expected from a linear mixing rule.

The temperature resistance of PLA can be improved by the addition of PMMA through an increase in the material glass

transition temperature. This effect was confirmed by dynamical mechanical analysis which indicated potential gains of 15 °C in temperature resistance at PMMA content of 50%. The crystallization of the PLA phase however is severely hindered by the presence of PMMA. Even though PLA always keep the theoretical ability to phase separate by crystallization, this process is so slow that for all practical purposes, the PLA/PMMA blend can be considered as a stable amorphous blend. This prevents using crystallization as an additional means to improve the temperature resistance of the material but enables retention of the transparency, which is a desired attribute in many instances.

Acknowledgements The authors would like to acknowledge the financial contribution of the Fond de recherche nature et technologie (FRQNT) of the province of Québec, Canada.

References

1. Auras R, Harte B, Selke S (2004) An overview of Poly(lactides) as packaging materials. *Macromol Biosci* 4(9):835–864. <https://doi.org/10.1002/mabi.200400043>
2. Flory PJ (1953) Principles of polymer chemistry. Cornell University Press, Ithaca
3. Anderson KS, Hillmyer MA (2004) The influence of block copolymer microstructure on the toughness of compatibilized poly(lactide)/poly(ethylene) blends. *Polymer* 45(26):8809–8823. <https://doi.org/10.1016/j.polymer.2004.10.047>
4. Choudhary P, Mohanty S, Nayak SK, Unnikrishnan L (2011) Poly(L-lactide)/polypropylene blends: evaluation of mechanical, thermal, and morphological characteristics. *J Appl Polym Sci* 121(6):3223–3237. <https://doi.org/10.1002/app.33866>
5. Sarazin P, Favis BD (2003) Morphology control in co-continuous poly (L-lactide)/polystyrene blends: a route towards highly structured and interconnected porosity in poly (L-lactide) materials. *Biomacromolecules* 4(6):1669–1679
6. Gajria AM, Davé V, Gross RA, McCarthy SP (1996) Miscibility and biodegradability of blends of poly(lactic acid) and poly(vinyl acetate). *Polymer* 37(3):437–444. [https://doi.org/10.1016/0032-3861\(96\)82913-2](https://doi.org/10.1016/0032-3861(96)82913-2)
7. Huneault MA, Li H (2007) Morphology and properties of compatibilized poly(lactide)/thermoplastic starch blends. *Polymer* 48(1):270–280. <https://doi.org/10.1016/j.polymer.2006.11.023>
8. Homklin R, Hongsriphan N (2013) Mechanical and thermal properties of PLA/PBS co-continuous blends adding nucleating agent. *Energy Procedia* 34:871–879. <https://doi.org/10.1016/j.egypro.2013.06.824>
9. Iannace S, Ambrosio L, Huang S, Nicolais L (1994) Poly (3-hydroxybutyrate)-co-(3-hydroxyvalerate)/poly-L-lactide blends: thermal and mechanical properties. *J Appl Polym Sci* 54(10):1525–1535
10. La Mantia FP, Botta L, Morreale M, Scaffaro R (2012) Effect of small amounts of poly(lactic acid) on the recycling of poly(ethylene terephthalate) bottles. *Polym Degrad Stab* 97(1):21–24. <https://doi.org/10.1016/j.polymdegradstab.2011.10.017>
11. McLauchlin AR, Ghita OR (2016) Studies on the thermal and mechanical behavior of PLA-PET blends. *J Appl Polym Sci* 133(43):n/a–n/a. <https://doi.org/10.1002/app.44147>
12. Hiljanen-Vainio M, Varpomaa P, Seppälä J, Törmälä P (1996) Modification of poly (L-lactides) by blending: mechanical and hydrolytic behavior. *Macromol Chem Phys* 197(4):1503–1523

13. Harada M, Iida K, Okamoto K, Hayashi H, Hirano K (2008) Reactive compatibilization of biodegradable poly(lactic acid)/poly(ϵ -caprolactone) blends with reactive processing agents. *Polym Eng Sci* 48(7):1359–1368. <https://doi.org/10.1002/pen.21088>
14. Yang J-M, Chen H-L, You J-W, Hwang JC (1997) Miscibility and crystallization of poly(L-lactide)/poly(ethylene glycol) and poly(L-lactide)/poly(ϵ -caprolactone) blends. *Polym J* 29(8):657–662
15. Sheth M, Kumar RA, Davé V, Gross RA, McCarthy SP (1997) Biodegradable polymer blends of poly(lactic acid) and poly(ethylene glycol). *J Appl Polym Sci* 66(8):1495–1505. [https://doi.org/10.1002/\(SICI\)1097-4628\(19971121\)66:8<1495::AID-APP10>3.0.CO;2-3](https://doi.org/10.1002/(SICI)1097-4628(19971121)66:8<1495::AID-APP10>3.0.CO;2-3)
16. Eguiburu JL, Iruin JJ, Fernandez-Berridi MJ, San Román J (1998) Blends of amorphous and crystalline polylactides with poly(methyl methacrylate) and poly(methyl acrylate): a miscibility study. *Polymer* 39(26):6891–6897. [https://doi.org/10.1016/S0032-3861\(98\)00182-7](https://doi.org/10.1016/S0032-3861(98)00182-7)
17. Zhang G, Zhang J, Wang S, Shen D (2003) Miscibility and phase structure of binary blends of polylactide and poly(methyl methacrylate). *J Polym Sci B Polym Phys* 41(1):23–30. <https://doi.org/10.1002/polb.10353>
18. Li S-H, Woo EM (2008) Effects of chain configuration on UCST behavior in blends of poly(L-lactic acid) with tactic poly(methyl methacrylate)s. *J Polym Sci B Polym Phys* 46(21):2355–2369. <https://doi.org/10.1002/polb.21567>
19. Li S-H, Woo EM (2008) Immiscibility–miscibility phase transitions in blends of poly(L-lactide) with poly(methyl methacrylate). *Polym Int* 57(11):1242–1251. <https://doi.org/10.1002/pi.2469>
20. Shirahase T, Komatsu Y, Tominaga Y, Asai S, Sumita M (2006) Miscibility and hydrolytic degradation in alkaline solution of poly(L-lactide) and poly(methyl methacrylate) blends. *Polymer* 47(13):4839–4844. <https://doi.org/10.1016/j.polymer.2006.04.012>
21. Le K-P, Lehman R, Remmert J, Vanness K, Ward PML, Idol JD (2006) Multiphase blends from poly(L-lactide) and poly(methyl methacrylate). *J Biomater Sci Polym Ed* 17(1–2):121–137. <https://doi.org/10.1163/156856206774879054>
22. Anakabe J, Zaldua Huici AM, Eceiza A, Arbelaz A (2015) Melt blending of polylactide and poly(methyl methacrylate): thermal and mechanical properties and phase morphology characterization. *J Appl Polym Sci* 132(42):n/a–n/a. <https://doi.org/10.1002/app.42677>
23. Samuel C, Raquez J-M, Dubois P (2013) PLLA/PMMA blends: a shear-induced miscibility with tunable morphologies and properties? *Polymer* 54(15):3931–3939. <https://doi.org/10.1016/j.polymer.2013.05.021>
24. Nishi T, Wang T (1975) Melting point depression and kinetic effects of cooling on crystallization in poly(vinylidene fluoride)-poly(methyl methacrylate) mixtures. *Macromolecules* 8(6):909–915
25. Canetti M, Cacciamani A, Bertini F (2014) Miscible blends of polylactide and poly(methyl methacrylate): morphology, structure, and thermal behavior. *J Polym Sci B Polym Phys* 52(17):1168–1177. <https://doi.org/10.1002/polb.23544>
26. Fischer EW, Sterzel HJ, Wegner G (1973) Investigation of the structure of solution grown crystals of lactide copolymers by means of chemical reactions. *Kolloid-Zeitschrift und Zeitschrift für Polymere* 251(11):980–990. <https://doi.org/10.1007/bf01498927>
27. Roovers J, Toporowski PM (1992) Rheological study of miscible blends of 1,4-polybutadiene and 1,2-polybutadiene (63% 1,2). *Macromolecules* 25(3):1096–1102. <https://doi.org/10.1021/ma00029a014>
28. RunMing L, Wei Y, ChiXing Z (2007) Phase inversion and viscoelastic properties of phase-separated polymer blends. *Polym Bull* 59(4):545–554. <https://doi.org/10.1007/s00289-007-0794-5>
29. Schnell M, Ziegler V, Wolf BA (2008) Evolution of viscosities and morphology for the two-phase system polyethylene oxide/poly(dimethylsiloxane). *Rheol Acta* 47(4):469–476. <https://doi.org/10.1007/s00397-007-0240-5>
30. Liu C, Wang J, He J (2002) Rheological and thermal properties of m-LLDPE blends with m-HDPE and LDPE. *Polymer* 43(13):3811–3818. [https://doi.org/10.1016/S0032-3861\(02\)00201-X](https://doi.org/10.1016/S0032-3861(02)00201-X)
31. Chopra D, Kontopoulou M, Vlassopoulos D, Hatzikiriakos GS (2002) Effect of maleic anhydride content on the rheology and phase behavior of poly(styrene-co-maleic anhydride)/poly(methyl methacrylate) blends. *Rheol Acta* 41(1):10–24. <https://doi.org/10.1007/s003970200001>
32. Sarkhel G, Banerjee A, Bhattacharya P (2006) Rheological and mechanical properties of LDPE/HDPE blends. *Polym Plast Technol Eng* 45(6):713–718. <https://doi.org/10.1080/03602550600609663>
33. Lodge TP, McLeish TCB (2000) Self-concentrations and effective glass transition temperatures in polymer blends. *Macromolecules* 33(14):5278–5284. <https://doi.org/10.1021/ma9921706>
34. Gordon M, Taylor JS (1952) Ideal copolymers and the second-order transitions of synthetic rubbers. i. Non-crystalline copolymers. *J Appl Chem* 2(9):493–500. <https://doi.org/10.1002/jctb.5010020901>
35. Jalali A, Huneault MA, Elkoun S (2016) Effect of thermal history on nucleation and crystallization of poly(lactic acid). *J Mater Sci* 51(16):7768–7779. <https://doi.org/10.1007/s10853-016-0059-5>
36. Saeidlou S, Huneault MA, Li H, Sammut P, Park CB (2012) Evidence of a dual network/spherulitic crystalline morphology in PLA stereocomplexes. *Polymer* 53(25):5816–5824. <https://doi.org/10.1016/j.polymer.2012.10.030>